NANO EXPRESS

Electrochemical properties of double wall carbon nanotube electrodes

Martin Pumera

Abstract Electrochemical properties of double wall carbon nanotubes (DWNT) were assessed and compared to their single wall (SWNT) counterparts. The double and single wall carbon nanotube materials were characterized by Raman spectroscopy, scanning and transmission electron microscopy and electrochemistry. The electrochemical behavior of DWNT film electrodes was characterized by using cyclic voltammetry of ferricyanide and NADH. It is shown that while both DWNT and SWNT were significantly functionalized with oxygen containing groups, double wall carbon nanotube film electrodes show a fast electron transfer and substantial decrease of overpotential of NADH when compared to the same way treated single wall carbon nanotubes.

Keywords Double wall carbon nanotube ·
Single wall carbon nanotube · Electrochemistry ·
Cyclic voltammetry · NADH

Introduction

Since the discovery of multi wall carbon nanotubes (MWNT) in 1991 by Iijima [1] and their single wall (SWNT) counterparts two years later [2], these nanoscale materials have attracted a vast interest because of

M. Pumera (✉)
ICYS, National Institute for Materials Science, 1-1 Namiki, Tsukuba, Ibaraki, Japan
e-mail: PUMERA.Martin@nims.go.jp

their unique chemical, mechanical and electronic properties [3]. Their interesting electrochemical properties have led in to explosive research activity in the field of carbon nanotube-based electrochemical sensors in the recent years [4–10]. Majority of the carbon nanotube-modified electrodes have been prepared by casting NT films on the surface of glassy carbon electrodes using multi wall or single wall carbon nanotubes [11–16]. While the electrochemical properties of MWNT and SWNT were studied recently, the information on electrochemical behavior of double wall carbon nanotubes (DWNT) is somehow missing despite the fact that DWNT may be interesting in many electrochemical applications since the outer wall could provide an interface with the rest of the system, while inner wall can act as 1D nanowire [17–20].

In this paper, I describe and characterize double wall carbon nanotube electrodes and assess their potential for electrochemical sensing. In the next sections I will describe that such DWNT electrodes have favorable electrochemical properties when compared to their SWNT counterparts which can lead to low-potential detection systems.

Experimental section

Apparatus

All voltammetric experiments were performed using an electrochemical analyzer μAutolabIII (Ecochemie, Utrecht, The Netherlands) connected to a personal computer and controlled by General Purpose Electrochemical Systems v. 4.9 software (Ecochemie). Electrochemical experiments were carried out in a 5 mL

voltammetric cell at room temperature (25 °C), using three electrode configuration. A platinum electrode served as an auxiliary electrode and an Ag/AgCl as a reference electrode. All electrochemical potential in this paper are stated vs. Ag/AgCl if not declared otherwise. Scanning electron microscope (SEM), field emission type, (Hitachi S-4800, Tokyo, Japan) was used to study the morphology of DWNT and SWNT films. JEM 2100F field emission transmission electron microscope (JOEL, Tokyo, Japan) working at 200 kV was used to acquire TEM figures in a scanning TEM mode (S/TEM; spot size, 0.7 nm; acceleration voltage, 200 kV). Raman spectra were collected using the 514.5 nm excitation from Ar ion laser beam in the backscattering geometry (BeamLok 2060-RS/T64000, Spectro-Physics, Mountain View, CA/Jobin Yvon, Horiba, France).

Materials

Double wall carbon nanotubes (DWNT, catalog no. 637351, purity >90%), single wall carbon nanotubes (SWNT, catalog no. 519308), nicotinamide adenine dinucleotide (reduced disodium salt hydrate) (NADH), potassium ferricyanide, potassium phosphate dibasic and phosphoric acid were purchased from Sigma-Aldrich (Japan).

Procedure

DWNT and SWNT nanotubes were functionalized with carboxyl groups in concentrated nitric acid (6 M) for 24 hours at 80°C [21–23]. The acid/NT mixture was subsequently washed with distilled water and centrifuged several times until their aqueous solution reached neutral pH. Subsequently, oxygen groups functionalized carbon nanotubes were filtered through 0.2 μm membrane (Nuclepore Track-Etch Membrane, Whatman, UK) using vacuum, creating carbon nanotube films (papers). DWNT and SWNT functionalized with carboxyl groups are referred in following text as DWNTox and SWNTox, while as-received carbon nanotubes as DWNTas and SWNTas.

For SEM measurements, the carbon nanotube films were adhered on conducting tape. For the electrochemistry measurements, the carbon nanotubes were cast onto the glassy carbon (GC) electrode surface, which was previously polished with 0.05 μm alumina on polishing cloth. Nanotubes were first dispersed in distilled water in concentration of 1 mg mL^{-1} and the suspension was then placed for 5 min into an ultrasonic bath, after which 5 μL of suspension was pipetted on electrode surface. It was allowed to evaporate at room temperature creating randomly distributed film on GC surface. Cyclic voltammetric experiments were carried out at a scan rate of 50 mV s^{-1} over relevant potential range using 50 mM phosphate buffer (pH 7.4). For TEM measurements, 1 μL of 1 mg mL^{-1} solution of NT was dropped on copper TEM grid and left to dry in air.

Results and discussion

Double wall carbon nanotubes and their single wall counterparts were characterized by Raman spectroscopy, scanning electron microscopy, transmission electron microscopy and cyclic voltammetry. Raman spectroscopy was used to estimate degree of functionalization of carbon nanotubes with carboxyl groups after treating them in nitric acid at elevated temperature. SEM served for imaging and comparison of morphology DW and SW nanotube films. TEM was used as another method to confirm the presence of DWNT and SWNT in the corresponding films. Cyclic voltammetry was employed for estimation of capacitance of nanotube layer and for examination of electrochemical response of ferricyanide/ferrocyanide and NADH on the DWNT and SWNT electrode films.

Raman spectroscopy

The double wall carbon nanotubes and their single wall counterparts were first oxidized by refluxing in nitric acid to produce carboxyl groups at the defect sites on their graphene sheet. Modifications of structure was identified by comparison of the Raman spectra of the as-received nanotubes (Fig. 1A and C for DWNTas and SWNTas, respectively) and the carboxyl group functionalized nanotubes (Fig. 1B and D for DWNTox and SWNTox, respectively) in the locality of the D band (disorder sp^3 band, around 1350 cm^{-1}) and G band (corresponding stretching mode in graphene plane, around 1580 cm^{-1}) of graphene sheet [22]. There is a significant increase of D-band intensity which is attributed to graphene sheet carbon sp^3 hybridization due to functionalization with oxygen containing groups; G/D ratio decreased from 11.3 for DWNTas to 2.8 for DWNTox, from 24.4 for SWNTas to 2.0 for SWNTox, reflecting strong functionalization of graphene sheet of both DW and SW carbon nanotubes with carboxyl containing groups.

Scanning electron microscopy

SEM microscopy was used to gain insight on the surface characteristics of carboxyl group functionalized
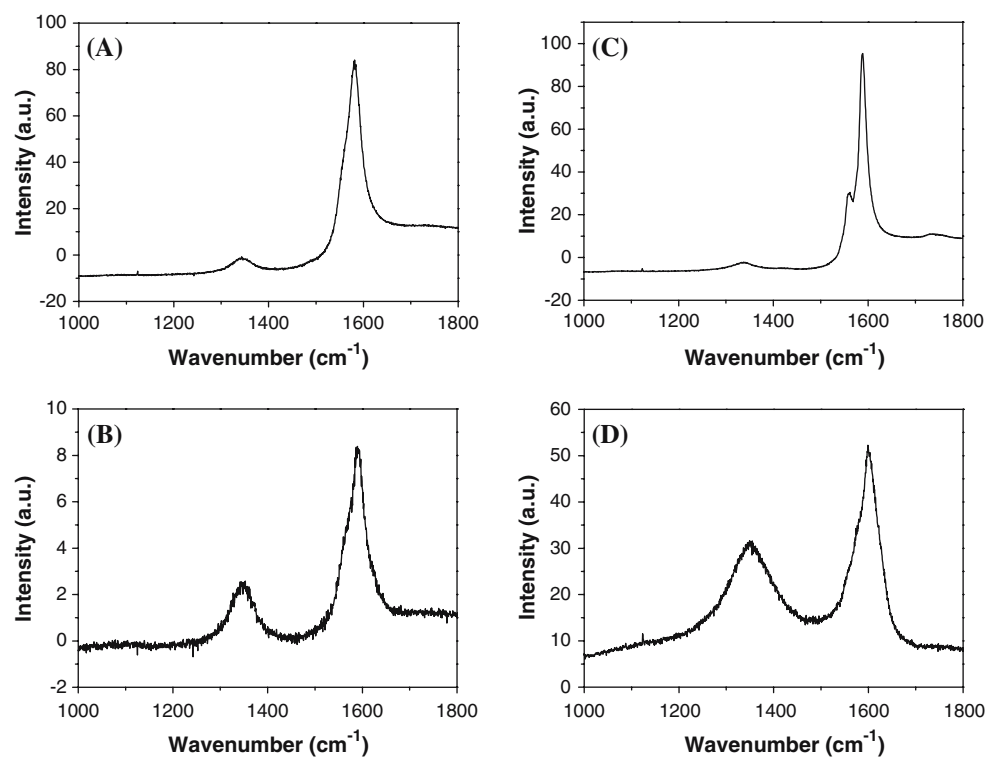
Fig. 1 Raman spectra of DWNTas (**A**), DWNTox (**B**), SWNTas (**C**) and SWNTox (**D**)

carbon nanotube films. Figure 2 compares SEM images of DWNTox (A, B) and SWNTox (C, D) films at different magnifications. SEM micrographs show very different surface morphologies of DWNTox and SWNTox films, which have strong impact on electrochemical behavior (capacitance) of the carbon nanotube film modified electrodes, as we will show in the following section "Capacitance Measurements". Surface of DWNTox film (A) is non-uniform, showing rough interwoven surface with feature size of 10–20 μm, while surface of SWNTox film (C) is very flat and uniform in such a scale, with very few defects. Note that the NT film can be broken when applying mechanical stress, as it is intentionally shown in both Figs. (A, C). The surface morphology of nanotube film is also very interesting on nanoscale level. Surface of DWNTox shows on 180 000× magnification (resolution 1–2 nm) interwoven bundles of double wall nanotubes (B). It is possible to see that surface of SWNTox film is very uniform even at such magnification and only when we focus on one of the rare defects in its surface it gives us insight to its inner structure (D). For comparison, SEM microscopy was used to study the morphology of as received DW and SW nanotube films (see Fig. S1, in Electronic Supplementary Material (ESM)). It is clear from these figures that the DWNTas and SWNTas provide more porous and rugged morphology, which

has direct effect upon their capacitance (see section "Capacitance Measurements" bellow).

Transmission electron microscopy

TEM images confirm the structures of DWNTox and SWNTox films observed by SEM in section "Scanning Electron Microscopy". DWNTox films contains interwoven nanotubes with spacing between them (Fig. 3A), where nanotubes are typically presented as individual structures (B). In contrary SWNTox creates interwoven densely packed nanotube mat (Fig. 3C), where nanotube ropes and occasionally individual single wall nanotubes sticking out from the mat at its borders (D). TEM investigation confirms the dimensions of nanotubes provided by their manufacturers, that inner diameter of DWNTox varies from 1.9 to 2.4 nm and outer from 2.6 to 3.1 nm, while diameter of SWNTox is about 1.2 nm.

Capacitance measurements

In order to gain information on capacitance of DWNTox and SWNTox film electrodes the background responses of the NT film electrodes in phosphate buffer were examined. The capacitance were calculated from plots of the current recorded at
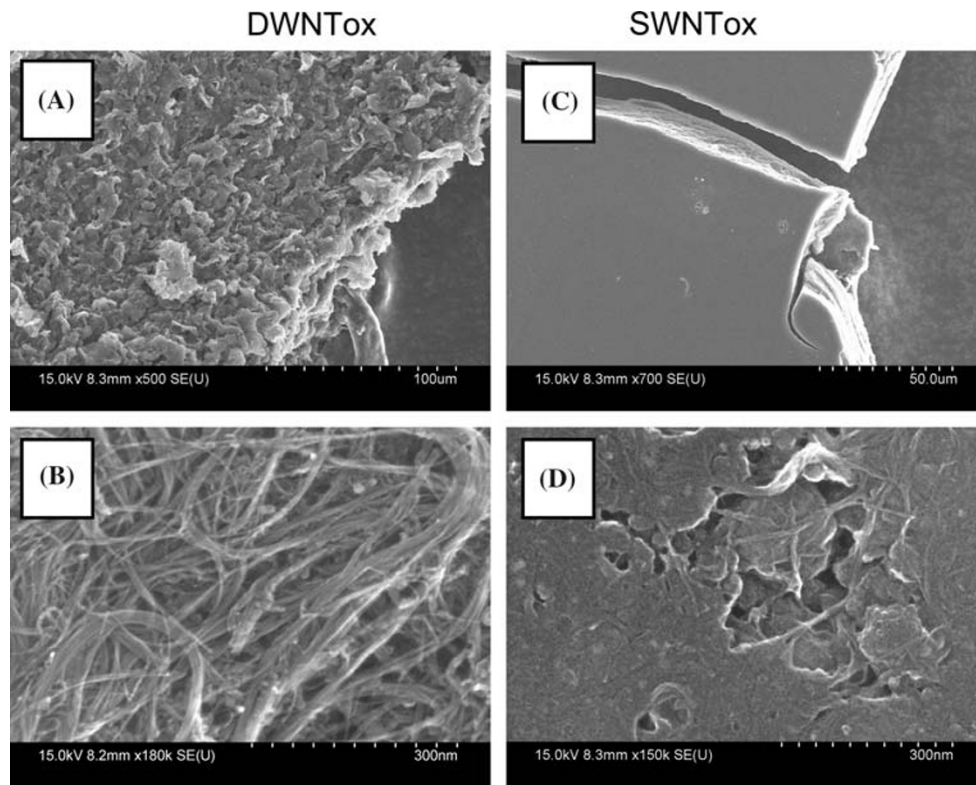
Fig. 2 SEM images of DWNTox (**A**, **B**) and SWNTox (**C**, **D**) films at low and high magnification
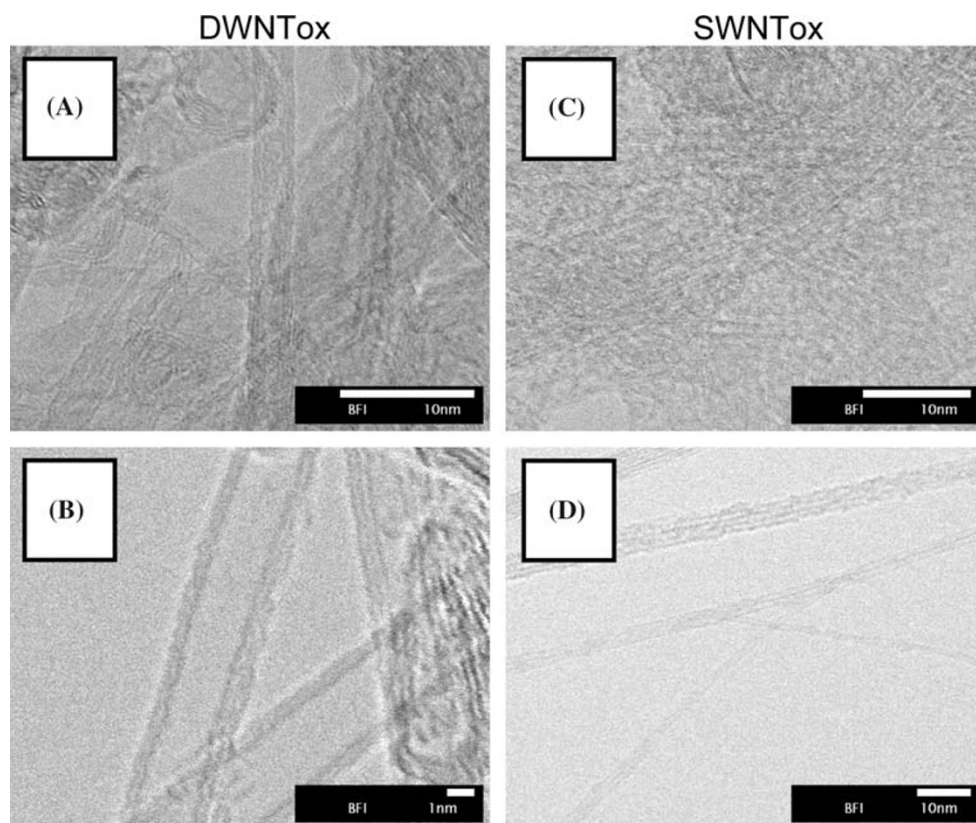
**Fig. 3** TEM images of DWNTox (**A**, **B**) and SWNTox (**C**, **D**) films at low and high magnification (acceleration voltage, 200 kV)

+0.40 V (vs. Ag/AgCl electrode) against the scan rate (varying from 25 mV s^{-1} to 200 mV s^{-1}) during cyclic voltammetry experiments in 50 mM phosphate buffer (pH 7.4; scan range from –200 mV to 1100 mV) on DWNTox and SWNTox film electrodes [13], see Fig. 4. These plots were linear in both cases which indicate that baseline current correspond directly to the capacitive charge/discharge current. The surface specific capacitances of DWNTox film electrode was found to be 25.86 μF mm^{-2} (and corresponding weight specific capacitance of 36.60 F g^{-1}), while capacitance of SWNTox was found to be 2.07 μF mm^{-2} (and corresponding weight specific capacitance of 2.93 F g^{-1}); capacitance of bare GC electrode was found to be 1.31 μF mm^{-2}. These data are coherent with SEM morphology observations which showed more rugged films with higher surface area in case of DWNTox, since the capacitance of the electrode originates from charging of double layer on electrode surface, which is proportionate to surface area [24]. To have a clear idea about the effect of nitric acid treatment upon capacitance of carbon NT film electrodes, capacitances of DWNTas and SWNTas film electrodes was also investigated and corresponding cyclic voltammograms in 50 mM phosphate buffer were measured; and corre-

sponding capacitances were obtained from plot of the current recorded at +0.40 V (vs. Ag/AgCl electrode) against the scan rate (see Fig. S2, ESM). The surface specific capacitance of DWNTas was found to be 55.40 μF mm^{-2} (and corresponding weight specific capacitance of 71.61 F g^{-1}), while the capacitance of SWNTas was found to be 20.25 μF mm^{-2} (and corresponding weight specific capacitance of 28.66 F g^{-1}). The higher capacitance for DWNTas and SWNTas vs. their carboxylic group functionalized counterparts originates from more porous and rugged surface of DWNTas and SWNTas films (compare SEM in Fig. 2 and Fig. S1 in ESM) therefore contains more surface area for charging of double layer. The difference between the observed capacitances of carbon NTox films are coherent with these published by Lawrence et al. for (acid treated) MWNTox films on GC electrodes [13] (recalculated weight specific capacitances of MWNTox films from Table 1 in Ref. [13] are ranging from 2.60 to 27.92 F g^{-1}) and these published by Li et al. for SWNT papers (weight specific capacitance of 16.9 F g^{-1}) [10]. The difference between weight specific capacitance of SWNTox films presented here (2.93 F g^{-1}) and in Ref [10] for SWNT papers (16.9 F g^{-1}) can be explained by the different
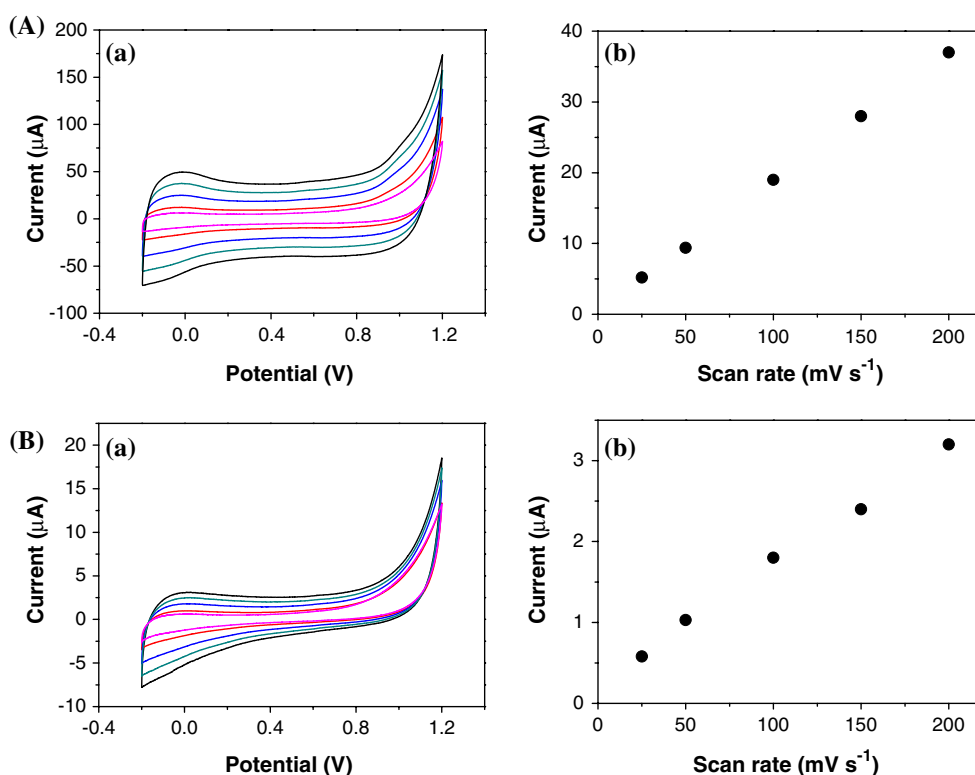
Fig. 4 (a) Cyclic voltammograms for the blank phosphate buffer (50 mM, pH 7.4) solution on DWNTox (**A**) and SWNTox (**B**) films. From inside voltammograms to outside ones, the scan rate is 25 mV s^{-1}, 50 mV s^{-1}, 100 mV s^{-1}, 150 mV s^{-1}, 200 mV s^{-1}. (b) Corresponding annodic currents of the cyclic voltammetry at +0.4 V for DWNTox (**A**) and SWNTox (**B**) films
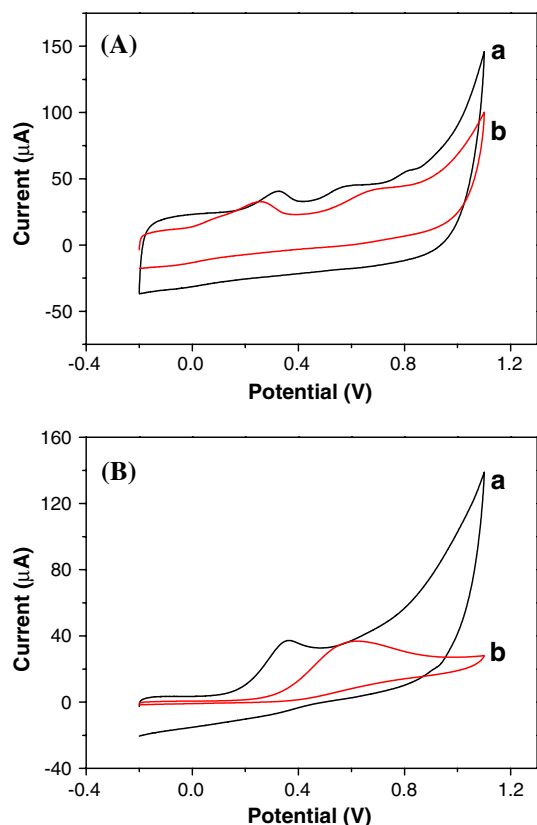
Fig. 5 Cyclic voltammogram of 5 mM NADH at DWNTas (**A**, a) and DWNTox (**A**, b); and SWNTas (**B**, a) and SWNTox (**B**, b) films coated GC electrode. Conditions: Scan rate, 50 mV s^{-1}; buffer, 50 mM phosphate, pH 7.4

morphology of the films and the higher number of individual SWNT in bundles in present work.

Cyclic voltammetry

To obtain information on resistivity of nanotube films, cyclic voltammograms for 5 mM ferricyanide at DWNTox and SWNTox film electrodes as well as at DWNTas and SWNTas were recorded in phosphate buffer (50 mM. pH 7.4) at 50 mV s^{-1} (see Fig. S3, ESM). The higher separation between the peak potentials (ΔE_p) is, the higher the resistivity of the NT film [8, 25] (ΔE_p is defined as difference between potential of anodic and cathodic peak, $E_{p,a}$ and $E_{p,c}$, respectively). Ferricyanide displays a reversible response on all DWNTox, DWNTas, SWNTox and SWNTas electrode films, with well defined peaks. The corresponding reductive to oxidative peak-to-peak separations (ΔE_p) for ferricyanide are 0.107 V at DWNTas and 0.111 V at DWNTox electrode films. This negligible difference between ΔE_p using DWNTas and DWNTox reflects that the conductivity (resp. resistivity) of DWNT after

oxidation did not significantly change and also that DWNTas and DWNTox provide fast electron transfer. However, in case of SWNT the results suggest that there is significant difference between resistivity of SWNTas and SWNTox films. ΔE_p of ferricyanide was found to increase from 0.095 V for SWNTas to 0.215 V for SWNTox, reflecting higher resistivity of SWNTox after their functionalization with carboxylic groups. This electrochemical behavior leads to the conclusion that while SWNTox are strongly oxidized (as seen from Raman spectra), their electronic structure receives a significant damage and there is increased resistivity of SWNTox. The CV experiments also suggest that while DWNTox are also strongly oxidized, their conductivity remains to be virtually the same since most likely only outer wall receives this oxidative damage. It is important to note that although it is favorable that the peak-to-peak separation of DWNT film changes little upon oxidation, the large peak separation of ~0.110 V in comparison to the closer-to-ideal peak-separation of 0.095 V suggests a slower electron transfer for the DWNTas in comparison to the as received SWNTas.

Next let's turn our attention to oxidation of nicotinamide adenine dinucleotide (NADH). NADH is important cofactor for more than 450 oxidoreductase enzymes [26] and for this reason its electrochemical oxidation has been frequently investigated. While the formal potential of the two electron oxidation of NADH to NAD$^+$ reaction is low (–0.56 V vs. SCE) [27], significant overpotential at bare electrodes is usually observed. Cyclic voltammetric experiments for oxidation of NADH indicated improved electrochemical reactivity towards oxidation of this molecule at DWNTox electrodes as compared to DWNTas film electrodes. DWNTox electrode displays two oxidation peaks for NADH, one well defined at +0.254 V and less defined second peak at +0.664 V (see Fig. 5A) while DWNTas films displays three oxidation peaks for NADH, first at +0.333 V, second very broad at +0.596 V and third at small peak at +0.814 V. These peaks are presented in CV reproducibly. It was suggested that the two wave response for NADH oxidation at MWNTox film modified glassy carbon electrodes is due to the different kinetics of NADH oxidation on edge plane sites of the CNTs and those of the underlying glassy carbon electrode [28]; this behavior is also consistent with other previous observation of electrochemistry of NADH at MWNTox/GC films [11, 13]. This conclusion is also supported by the observation of NADH single oxidation peak at bare GC electrode at +0.645 V in this work which corresponds to the second wave. The presence of the third small oxidation wave of NADH in case of as received

DWNTas (it means un-purified) film electrode is most likely due to presence of other electrochemically active material (with different oxidation kinetics for NADH) in the as received DWNTas sample which was removed by oxidation with concentrated HNO_3 at elevated temperature. It is clear that DWNTox electrode provide more favorable electrochemistry and reducing of overpotential of NADH oxidation than DWNTas film electrode. It was shown that reducing overpotential of NADH oxidation is related to introducing defects on carbon nanotube walls [25] and to nanotube open-ends which are similar to the edge-plane of highly oriented pyrolytic graphite [12]. Such a decrease in oxidation potentials of NADH at DWNTox films (compared to DWNTas) suggests that the inner graphene layer of DWNTox is intact and serving as nanowire to carry electrons to the electrode surface while heavily oxidized outer graphene of DWNTox is providing sites for electrocatalytic oxidation of NADH.

The electrochemical behavior of SWNTox films towards oxidation of NADH is consistent with SWNTox film oxidation of ferricyanide and it is very different in respect to behavior of DWNT films. The SWNTox film modified electrode shows oxidation peak of NADH at significantly high potential of +0.591 V (vs. Ag/AgCl) (see Fig. 5B) while as-received SWNTas provide oxidation peak of NADH at lower potential of +0.386 V (note very slight second oxidation peak about ~0.650 V), reflecting higher resistivity of oxidized SWNTox comparing to SWNTas.

It is important to note that while SWNTox and DWNTox were treated the same way in this study and received similar amount of oxidative wall damage (as shown by Raman spectroscopy in section ''Raman Spectroscopy''), the electrochemistry suggests that the inner graphene layer of DWNTox is intact and serving as 1D nanowire while heavily oxidized and damaged outer graphene of DWNTox is providing sites for electrocatalytic oxidation of NADH. This ''dual'' feature is clearly not available in case of SWNTox.

Conclusion

For the first time, the electrochemical utility of double wall carbon nanotube was demonstrated. The results presented above reveals that outer wall of oxidized double wall carbon nanotube can provide active sites for effective oxidation of biomolecules while inner wall of nanotube acts as 1D nanowire. This property is similar to the one found in the multiwall carbon nanotubes, however, double wall nanotubes provide much smaller diameter. Double wall carbon nanotubes should find a wide range application in area of nanobiosensors and nanobioelectronics, as nanoelectrodes or AFM tips.

References

1. S. Iijima, Nature **354**, 56 (1991)
2. S. Iijima, T. Ichihashi, Nature **363**, 603 (1993)
3. P. M. Ajayan, Chem. Rev. **99**, 1787 (1999)
4. J. Wang, Electroanal **17**, 7 (2005)
5. J.J. Gooding, Electrochim. Acta **50**, 3049 (2005)
6. M. Pumera, S. Sanchez, I. Ichinose, J. Tang, Sensors Actuators B, in press, doi: 10.1016/j.snb.2006.11.016
7. A. Merkoci, M. Pumera, X. Llopis, B. Perez, M. del Valle, S. Alegret, Trends Anal. Chem. **24**, 826 (2005)
8. M. Pumera, A. Merkoci, S. Alegret, Sens. Actuators B **113**, 617 (2006)
9. B. Perez, M. Pumera, M. del Valle, A. Merkoci, S. Alegret, J. Nanosci. Nanotech. **5**, 1694 (2005)
10. J. Li, A. Cassell, L. Delzeit, J. Han, M. Meyyappan, J. Phys. Chem. B **106**, 9299 (2002)
11. M. Musameh, J. Wang, A. Merkoci, Y. Lin, Electrochem. Commun. **4**, 743 (2002)
12. R.R. Moore, C.E. Banks, R.G. Compton, Anal. Chem. **76**, 2677 (2004)
13. N.S. Lawrence, R.P. Deo, J. Wang, Electroanal **17**, 65 (2005)
14. C.E. Banks, R.R. Moore, T.J. Davies, R.G. Compton, Chem. Commun. **16**, 1804 (2004)
15. N.S. Lawrence, R.P. Deo, J. Wang, Electrochem. Commun. **6**, 176 (2004)
16. M. Pumera, X. Llopis, A. Merkoci, S. Alegret, Microchim. Acta **152**, 261 (2006)
17. M. Endo, T. Hayashi, H. Muramatsu, Y.-A. Kim, H. Terrones, M. Terrones, M. S. Dresselhaus, Nano Lett. **4**, 1451 (2004)
18. E. Flahaut, A. Peigney, C. Laurent, J. Nanosci. Nanotech. **3**, 151 (2003)
19. S. Wang, M. Grifoni, Phys. Rev. Lett. **95**, 266802 (2005)
20. W. Ren, F. Li, J. Chen, S. Bai, H.-M. Cheng, Chem. Phys. Lett. **359**, 196 (2002)
21. A. Gomathi, S.R.C. Vivekchand, A. Govindaraj, C.N.R. Rao, Adv. Mater. **17**, 2757 (2005)
22. K. Kordas, T. Mustonen, G. Toth, H. Jantunen, M. Lajunen, C. Soldano, S. Talapatra, S. Kar, R. Vajtai, P.M. Ajayan, Small **2**, 1021 (2006)
23. X. Yu, B. Munge, V. Patel, G. Jensen, A. Bhirde, J.D. Gong, S.N. Kim, J. Gillespie, J.S. Gutkind, F. Papadimitrakopoulos, J.F. Rusling, J. Am. Chem. Soc. **128**, 11199 (2006)
24. A.J. Bard, L.R. Faulkner, *Electrochemical Methods: Fundamentals and Applications*, Chapter 1, (Wiley, 2000)
25. F. Valentini, A. Amine, S. Orlanducci, M.L. Terranova, G. Palleschi, Anal. Chem. **75**, 5413 (2003)
26. H.B. White, in *The Pyridine Nucleotide Cofactors*, ed. by J. Everse, B. Anderson, K.-S. You (Academic Press, New York, 1982), pp. 1-17
27. H.K. Chenault, G.M. Whitesides, Appl. Biochem. Biotechnol. **14**, 147 (1987)
28. C.E. Banks, R.G. Compton, Analyst **130**, 1232 (2005)